RSC Advances

ROYAL SOCIETY OF CHEMISTRY

www.rsc.org/advances

Pd-doped single-walled carbon nanotube as a nanobiosensor for histidine amino acid, a DFT study

Mehdi Yoosefian*[a], Nazanin Etminan[b]

[a] Department of Chemistry, Graduate University of Advanced Technology, Kerman, Iran

[b] Department of Chemistry, University of Payam-noor, Tehran, Iran

Abstract

Using DFT calculations, we investigate Pd-doped single walled carbon nanotube (Pd/SWCNT) as a bionanosensor platform for histidine amino acid detection. The adsorption features of three special adsorption sites of histidine molecule close to the Pd atom of nanotube that are all different from one another are fully optimized. The chemical properties, NBO and QTAIM analysis have been carried out to study the order of bonding strength in complexes and deep understanding of the nature of interactions in His-Pd/SWCNT. Chemical potential and hardness as the parameters that reflected the chemical reactivity and stability were calculated by DFT/B3LYP with 6-31G* basis set and DGDZVP extra basis set for Pd atom. Our results demonstrate that Pd/SWCNTs with the large binding energy and significant charge transfer through the adsorption of histidine amino acid can serve as a bionanosensor.

Keywords: histidine; Pd-doped SWCNT; bionanosensor; chemical properties.

1. Introduction

When Richard Phillips Feynman [1], the American theoretical physicist, said: "There is Plenty of Room at the Bottom", no one could imagine the novel and remarkable technological applications of different forms of crystalline carbons. Carbon nanotubes observation report by Dr. Sumio

* Corresponding author. Tel.: +98342622612; fax: +983426226617.

E-mail address: myoosefian@kgut.ac.ir (Mehdi Yoosefian).

Iijima [2] resulted in the worldwide development of an entirely new material field. CNTs are atomically well–defined cylindrical structures, with high mechanical stiffness and strength, low dimension and high surface to volume ratio [3]. Depending on their chirality, nanotubes can be metallic, semiconducting or semi metallic which exhibit different electrical and optical properties. Due to their unique properties, many novel applications have been demonstrated including electronics, optoelectronics, drug delivery shuttles, composites, sensors, and more [4-6]. Sensing molecules are critical to environmental monitoring, medical applications and controlling of chemical processes. Electrical sensors such as semiconducting metal oxides, silicon devices, organic materials and polymer composites exhibit limitations because they operate at high temperature and have limited sensitivity so individual single-walled carbon nanotubes (SWCNTs) proposed as new chemical sensors by Kong et al. to detect toxic gases and other species [7]. All of the carbon atoms on the SWNTs surface are highly sensitive to their environment. Because of the weak Van der Waals interaction of the intrinsic CNTs with the adsorbent, transition metal functionalized SWCNT as a super molecular ligand could be able to detect many biological molecules. Carbon nanotubes can be functionalized both covalently and non-covalently, but as the SP^2 structure preserves in non-covalent one, they found to be very sensitive to their environment. Embedding or doping (heteroatom substitution) of foreign atoms can modify and enhance the selectivity and sensitivity of SWCNTs due to different interaction of dopant and biological molecules[8-12]. Between the hallow site, bridge site and top site of SWCNT, doping the transition metal on the latest has the minimum energy and so is the stable one [13]. Strong binding energy and electron charge transfer are two important characteristics for a good sensor that depends on different adsorption features including physisorption, chemisorption and electrostatic [14-19]. The chemical and electrical properties of nanomaterials such as carbon nanotubes, metal nano particles and hybrid carbon/metal nanoparticle structures enhanced the biosensors performance. Usually the diameter of a SWCNT is <2nm and the length/diameter ratio can be as large as 10^4-10^5 nm so good biocompatibility of hybrid carbon/metal nanoparticle among the wide range of the nanomaterial makes them as a novel biosensor.

Biosensors are highly valuable devices for measuring a wide spectrum of analytes including organic compounds, gases, ions and bacteria [20]. A biosensor is an analytical device, used for detection of an analyte that combines a biological component with a physicochemical detector.

Attachment of the biological elements (small molecules/protein/cells) to the surface of the sensor is an important part in a biosensor. The main requirements for a biosensor approach to be valuable in terms of research and commercial applications are the identification of a target molecule, availability of a suitable biological recognition element, and the potential for disposable portable detection systems to be preferred to sensitive laboratory-based techniques in some situations [21]. Proteins are the major structural components of all cells in the body which could be detected by a biosensor. Proteins also function as enzymes, in membranes, as transport carriers, and as hormones. They consist of chains of amino acid subunits joined together by peptide bonds. Determination of amino acids is important in different fields of research, particularly in food and biotechnology. Histidine is an α-amino acid with an imidazole functional group and it is one of the 23 proteinogenic amino acids. Histidine is an essential amino acid in humans and other mammals [22]. It long has been recognized as a scavenger of the hydroxyl radical and of singlet oxygen, a biologically important non radical toxic oxygen species that is highly reactive because of an excited electron promoted to a higher energy orbital. Histidine appears to interact chemically with these toxic oxygen species through at least two distinct mechanisms:

(1) By interfering with the redox reactions involving metal ions that produce the hydroxyl radical and (2) By direct interactions of the histidine imidazole rings with singlet oxygen. Histidinemia is a rare hereditary metabolic disorder characterized by a deficiency of the enzyme histidase, which is necessary for the metabolism of the amino acid histidine. The concentration of histidine is elevated in the blood. Excessive amounts of histidine, imidazole pyruvic acid, and other imidazole metabolism products are excreted in the urine. The majority of individuals with histidinemia have no obvious symptoms that would indicate that a person has this disorder (asymptomatic). The aim of the present theoretical study is to design a novel biosensor with fast response time and high sensitivity to biological substances. To our knowledge, SWCNTs haven't been used as a biosensor for histidine biomolecule yet, so we introduce pd-doped SWCNT (Pd/SWCNT) to gain this purpose. The burgeoning field of nanobiosensors was because of the same length order of magnitude scale of many of the fundamental building blocks of life with nano scale material. Nanomaterial based biosensors with high sensitivities, low detection limit and short response time (<10 s) are good candidates for biosensing applications.

2. Models and computational details

The electronic properties of the Pd/SWCNT bionanosensor were studied by performing theoretical calculations with GAUSSIAN 03 Software package [23]. Pd-doped single-wall armchair (5,5) carbon nanotube ($C_{69}H_{20}Pd$) with open edges which its diameter and the bond length of Pd with three nearest C atom are 7.15, 2.06, 1.97 and 1.97 respectively, were considered. The optimized structure parameters of the SWCNT, Pd/SWCNT and the His-Pd/SWCNT calculated by ab initio (HF) and density functional calculation (DFT) with Beck's three parameter hybrid method using the correlation functional of Lee, Yang, Parr (B3LYP) level. Different basis sets were tested and all geometry full optimization have been performed with hybrid density functional B3LYP/6-31G* and DGDZVP extra basis set for Pd atom. Frequency calculations were also performed with the same basis set and since no imaginary frequencies were found, the optimized structures correspond to the energy minima. The characteristics of the bond critical points (BCP) and ring critical points (RCP) were analyzed in terms of the electron density at the critical point ρ_C and it's Laplacian.

Adsorption energy (E_{ads}) between histidine and Pd/SWCNT was defined as:

$$E_{ads} = E_{His\text{-}Pd/SWCNT} - E_{Pd/SWCNT} - E_{His} \quad (1)$$

Where $E_{His\text{-}Pd/SWCNT}$ is the total energy of the Pd/SWCNT with histidine molecule and $E_{Pd/SWCNT}$ and E_{His} are the total energy of Pd/SWCNT and histidine molecule in relax geometry respectively. Negative adsorption energy indicates the stable formed complexes and the positive adsorption energy referred to the local minima. To reduce the unfavorable interactions, histidine molecule was located at the perpendicular direction to the SWCNT. The interaction of histidine with Pd/SWCNT via different initial configurations complexes i.e. carbonyl, amine and imidazole ring were considered for each Pd-doped SWCNT complexes. These interactions change the conductivity of SWCNT through a charge transfer between lone pairs of Pd and the adsorbent, so to estimate sensing capacity, Natural Bond Orbital (NBO) analysis were performed for partial and net charge transfer.

Two important quantitative quantum chemical properties i.e chemical potential (μ); the first derivation of E and hardness (η); the second derivative of E are also studied in molecular systems. According to Koopsmans theorem:

$$\mu = \left(\frac{\partial E}{\partial N} \right)_{V(r),T} \quad (1)$$

$$\eta = \left(\frac{\partial^2 E}{\partial N^2} \right)_{V(r),T} \quad (2)$$

$$\varepsilon_F = \mu \quad (3)$$

Where E is the total electron energy, N is the number of electrons; V(r) is the external potential, and ε_H, ε_L , ε_F are the orbital energy of HOMO and LUMO and Fermi level respectively. The orbital energies of HOMO and LUMO orbitals and the energy gap between them were obtained from DFT calculations.

3. Result and discussion

3.1. Molecular configuration

In this paper we aim to present a detailed description of the character of binding between histidine amino acid and the Pd/SWCNT as a bionanosensor. Transition metal doped SWCNTs had shown high binding energy and magnetic ground states. According to the previous reports [24], because of the much stronger interaction of Pd and C-defective SWCNT, P-doped SWCNT geometry have been optimized as a bionanosensing platform.

The structures of Pd/SWCNT complexes were obtained using DFT method at the B3LYP level of theory. The optimized structure of the Pd/SWCNT from the side and top views are shown in Fig.1 in which a central C atom in the wall of CNT is replaced by a Pd atom. The Pd center was bounded to three carbon atoms and because of the much larger Pd atomic radius than that of carbon atom, Pd protrudes out off the wall surface which the Pd-C bond lengths are 2.063, 1.974 and 1.974.

The optimized geometry of histidine depicted in Fig. 2. By introducing the histidine molecule, the structure of Pd/SWCNT has not been distorted. For His-Pd/SWCNT system, we have investigated various possible adsorption geometries and to reduce the unfavorable interactions and steric effects, the initial configuration of histidine molecule was perpendicular to the axial direction of SWCNT.

Three special adsorption sites of histidine molecule close to the Pd site of nanotube are full optimized and labeled by panels A, B, C with amine, carbonyl and ring site respectively from top view and D, E, F from the side view were shown in Fig 3.

We have observed that Pd/SWCNT have distinguishable response to histidine amino acid. Therefore, evaluation of sensing mechanism of histidine onto Pd/SWCNT might fabricate nanotube based biosensor devise. All geometrical data indicates that the geometrical structures of Pd/SWCNT present changes caused from the adsorption.

The energetic properties of different complexes, which are important criterion for evaluation of a molecular biosensor result from the adsorption of His on Pd/SWCNT and other selected geometrical data, are listed in Table 1-3. The values of adsorption energies for the amine adsorption sites, complex 1, carbonyl site, complex 2 and ring site, complex 3, are -18.210 eV, -18.059 eV and -17.572 eV respectively. The negative sign of adsorption energy correspond to local minima stable complexes and the large adsorption energy suggests that chemisorption of histidine via amine site appears to be more stable than the adsorption of the other sites.

3.2 HOMO-LUMO analysis

Frontier molecular orbital plays an important role in electric properties. The orbital energies of the highest occupied molecular orbital (HOMO) and the lowest unoccupied molecular orbitals (LUMO) are the essential part of quantum mechanics that represent the stability of donor and acceptor through the electron transition-adsorption process. HOMO tends to give electron such an electron donor and LUMO contain free locations to accept electron and the energy gap between them reveals the electron conductivity and a measure of the structural stability properties. Fig. 4 showed the plot of different studied HOMO and LUMO orbitals of title sites.

The E_{HOMO}, E_{LUMO} and the energy gap between them, chemical potential, μ, chemical hardness, η, and Fermi level energy, ε_F, for different investigated configurations are presented in Table 4. The HOMO-LUMO energy gap for Pd/SWCNT is 1.6116 (eV) and after the adsorption on histidine via ring, amine and carbonyl site increases.

When the energy falls as the distance between the His and Pd/SWCNT decrease, the HOMO is going down in energy and LUMO is going up in energy and the small HOMO-LUMO energy

gap would result in increase of conductance of the nanotube through the charge transfer interaction.

3.3. QTAIM analysis

More details about the nature of interactions in His-Pd/SWCNT are obtained from the Bader's quantum theory of atoms in molecules (QTAIM) [25]. Bond paths, the direct connection trajectory between two atoms, bond critical points (BCP), the point with minimum charge density value along the bond path, bond ring critical points (RCP) and electron density distribution function that obtained from QTAIM computations would allow us to study the strength and chemical properties of bonds[26-34]. The negative sign of Laplacian of electron density at BCP demonstrates the domination of potential energy (covalent interactions) in the shared system, whereas the positive sign shows the domination of kinetic energy in closed shell interactions (van der Waal or ionic interactions). According to the performed calculations, given in Table 1-3, charge density at Pd-N bond in complex 1 in comparison to charge density at Pd-O and Pd-N bond in complex2 and complex 3 respectively, were increased showing the strong strength bond in Pd-N in adsorbed histidine on Pd/SWCNT. Furthermore, the positive sign of Laplacian for Pd-X (X=O, N, C, H atoms of histidine molecule) in all structures were illustrated the closed-shell interaction such as ionic and van der Waals interactions.

3.4. NBO analysis

Natural Bond Orbital (NBO) [35] gives information about the interactions that could be used to analysis molecular interactions [36-44]. The second-order perturbation stabilization energies, $E^{(2)}$, was calculated to evaluate the donor-acceptor interaction in NBO analysis and charge transfer or conjugate interaction in complex systems. Table 5 provides the result of the NBO analysis for His-Pd/SWCNT complexes containing the donor-acceptor interactions.

The results show that in complex1 lone pairs of pd participate as an acceptor and lone pair of N as a donor, meanwhile in complex 2 and complex 3 lone pairs of O and ring N are as the most important donors.

4. Conclusion

First principle calculations based on density functional theory (DFT) have been performed on the geometric structures and electronic properties of Pd-doped SWCNT. Transition metal doped SWCNT improved the sensing performance of SWCNT and make a good adsorbent candidate for the adsorption of histidine molecule. The adsorption characteristics of histidine molecule on Pd/SWCNT have been investigated. The biocompatible complex 2 with the amine site close to the Pd atom of the SWCNT, with the largest value of E_{ads}, would be important for fundamental researches and technical applications to develop Pd-doped SWCNT/his hybrid biosensor.

Acknowledgments:

The authors wish to thank Graduate University of Advanced Technology, Kerman, Iran, for their support. Also the technical support of the chemistry computational center at Shahid Beheshti University is gratefully acknowledged.

References

1. R. P. Feynman, *Miniaturization"(HD Gilbert, ed.) Reinhold, New York*, 1961.
2. S. Iijima, *nature*, 1991, 354, 56-58.
3. V. L. Pushparaj, M. M. Shaijumon, A. Kumar, S. Murugesan, L. Ci, R. Vajtai, R. J. Linhardt, O. Nalamasu and P. M. Ajayan, *Proceedings of the National Academy of Sciences*, 2007, 104, 13574-13577.
4. P. Avouris and J. Chen, *Materials Today*, 2006, 9, 46-54.
5. H. Dai, A. Javey, E. Pop, D. Mann, W. Kim and Y. Lu, *Nano*, 2006, 1, 1-13.
6. J. L. Blackburn, T. M. Barnes, M. C. Beard, Y.-H. Kim, R. C. Tenent, T. J. McDonald, B. To, T. J. Coutts and M. J. Heben, *Acs Nano*, 2008, 2, 1266-1274.
7. J. Kong, N. R. Franklin, C. Zhou, M. G. Chapline, S. Peng, K. Cho and H. Dai, *Science*, 2000, 287, 622-625.
8. C. Rajesh, C. Majumder, H. Mizuseki and Y. Kawazoe, *The Journal of chemical physics*, 2009, 130, 124911.
9. T. Zhang, S. Mubeen, N. V. Myung and M. A. Deshusses, *Nanotechnology*, 2008, 19, 332001.
10. S. Peng and K. Cho, *Nano Letters*, 2003, 3, 513-517.
11. P. Qi, O. Vermesh, M. Grecu, A. Javey, Q. Wang, H. Dai, S. Peng and K. Cho, *Nano letters*, 2003, 3, 347-351.
12. J. Kong, M. G. Chapline and H. Dai, *Advanced Materials*, 2001, 13, 1384-1386.
13. X. Zhou, W. Q. Tian and X.-L. Wang, *Sensors and Actuators B: Chemical*, 2010, 151, 56-64.
14. R. N. Goyal, V. K. Gupta, N. Bachheti and R. A. Sharma, *Electroanalysis*, 2008, 20, 757-764.
15. R. N. Goyal, V. K. Gupta and N. Bachheti, *Analytica Chimica Acta*, 2007, 597, 82-89.

16. R. N. Goyal, V. K. Gupta and S. Chatterjee, *Talanta*, 2008, 76, 662-668.
17. M. Yoosefian, H. Raissi and A. Mola, *Sensors and Actuators B: Chemical*, 2015, 212, 55-62.
18. R. Wang, D. Zhang, W. Sun, Z. Han and C. Liu, *Journal of Molecular Structure: THEOCHEM*, 2007, 806, 93-97.
19. V. K. Gupta, A. K. Jain and S. K. Shoora, *Electrochimica Acta*, 2013, 93, 248-253.
20. T. Vo-Dinh and B. Cullum, *Fresenius' journal of analytical chemistry*, 2000, 366, 540-551.
21. J. C. Pickup, Z. L. Zhi, F. Khan, T. Saxl and D. J. Birch, *Diabetes/metabolism research and reviews*, 2008, 24, 604-610.
22. R. Katoh, *Chemistry Letters*, 2007, 36, 1256-1257.
23. M. Frisch, G. Trucks, H. Schlegel, G. Scuseria, M. Robb, J. Cheeseman, J. Montgomery Jr, T. Vreven, K. Kudin and J. Burant, *Gaussian Inc., Wallingford, CT*, 2004.
24. M. Yoosefian, Z. Barzgari and J. Yoosefian, *Structural Chemistry*, 2014, 25, 9-19.
25. R. F. Bader, A. Streitwieser, A. Neuhaus, K. E. Laidig and P. Speers, *Journal of the American Chemical Society*, 1996, 118, 4959-4965.
26. V. C. Jordan, *Nat Rev Cancer*, 2007, 7, 46-53.
27. H. Raissi, F. Farzad, E. S. Nadim, M. Yoosefian, H. Farsi, A. Nowroozi and D. Loghmaninejad, *International Journal of Quantum Chemistry*, 2012, 112, 1273-1284.
28. H. Raissi, M. Yoosefian, A. Hajizadeh, M. KARIMI and F. FARZAD, *Bulletin of the Chemical Society of Japan*, 2012, 85, 87-92.
29. M. Yoosefian, H. Raissi, E. Davamdar, A. Esmaeili and M. Azaroon, *Chinese Journal of Chemistry*, 2012, 30, 779-784.
30. J. L. Borgna and H. Rochefort, *J Biol Chem*, 1981, 256, 859-868.
31. M. Yoosefian, H. Raissi, E. S. Nadim, F. Farzad, M. Fazli, E. Karimzade and A. Nowroozi, *International Journal of Quantum Chemistry*, 2011, 111, 3505-3516.
32. H. Raissi, A. Jalbout, M. Yoosefian, M. Fazli, A. Nowroozi, M. Shahinin and A. De Leon, *International Journal of Quantum Chemistry*, 2010, 110, 821-830.
33. H. Raissi, A. Jalbout, M. Fazli, M. Yoosefian, H. Ghiassi, Z. Wang and A. De Leon, *International Journal of Quantum Chemistry*, 2009, 109, 1497-1504.
34. H. Raissi, M. Yoosefian and F. Mollania, *Computational and theoretical chemistry*, 2012, 996, 68-75.
35. E. Glendening, A. Reed, J. Carpenter and F. Weinhold, 2003.
36. M. Yoosefian, Z. Jafari Chermahini, H. Raissi, A. Mola and M. Sadeghi, *Journal of Molecular Liquids*, 2015, 203, 137-142.
37. H. Raissi, M. Yoosefian, S. Zamani and F. Farzad, *Journal of Sulfur Chemistry*, 2012, 33, 75-85.
38. H. Raissi, M. Yoosefian, S. Zamani and F. Farzad, *JOURNAL OF SULFUR CHEMISTRY*, 2012, 33, 75-85.
39. H. Raissi, M. Yoosefian and S. Khoshkhou, *Computational and Theoretical Chemistry*, 2012, 983, 1-6.
40. H. Raissi, M. Yoosefian and F. Mollania, *International Journal of Quantum Chemistry*, 2012, 112, 2782-2786.
41. M. Fazli, A. Jalbout, H. Raissi, H. Ghiassi and M. Yoosefian, *Journal of Theoretical and Computational Chemistry*, 2009, 8, 713-732.

42. H. Raissi, A. Khanmohammadi, M. Yoosefian and F. Mollania, *Structural Chemistry*, 2013, 24, 1121-1133.
43. H. Raissi, M. Yoosefian, F. Mollania, F. Farzad and A. R. Nowroozi, *Computational and Theoretical Chemistry*, 2011, 966, 299-305.
44. E. S. Nadim, H. Raissi, M. Yoosefian, F. Farzad and A. R. Nowroozi, *Journal of Sulfur Chemistry*, 2010, 31, 275-285.

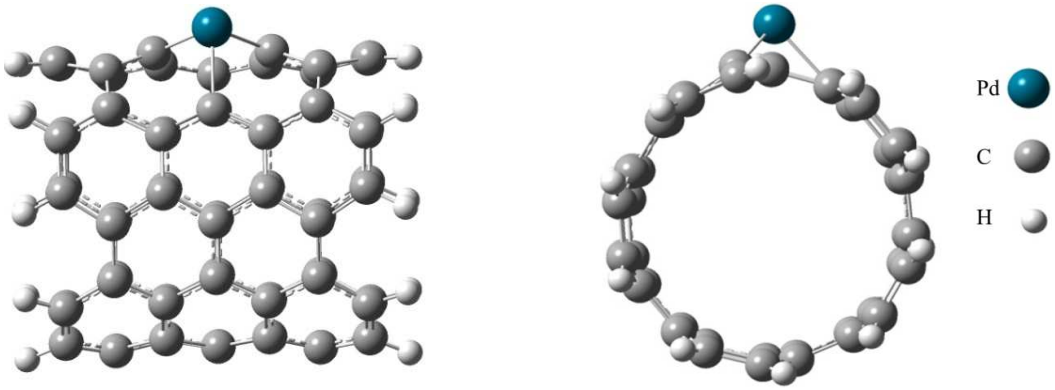

(a) (b)

Fig. 1.

Optimized structure of Pd/SWCNT from (a) side view and (b) top view

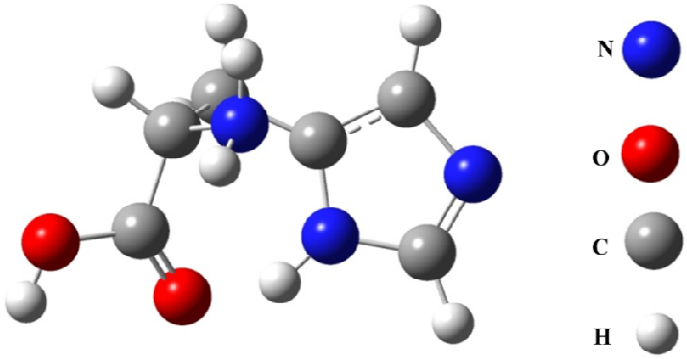

Fig. 2.

Optimized geometry of histidine molecule

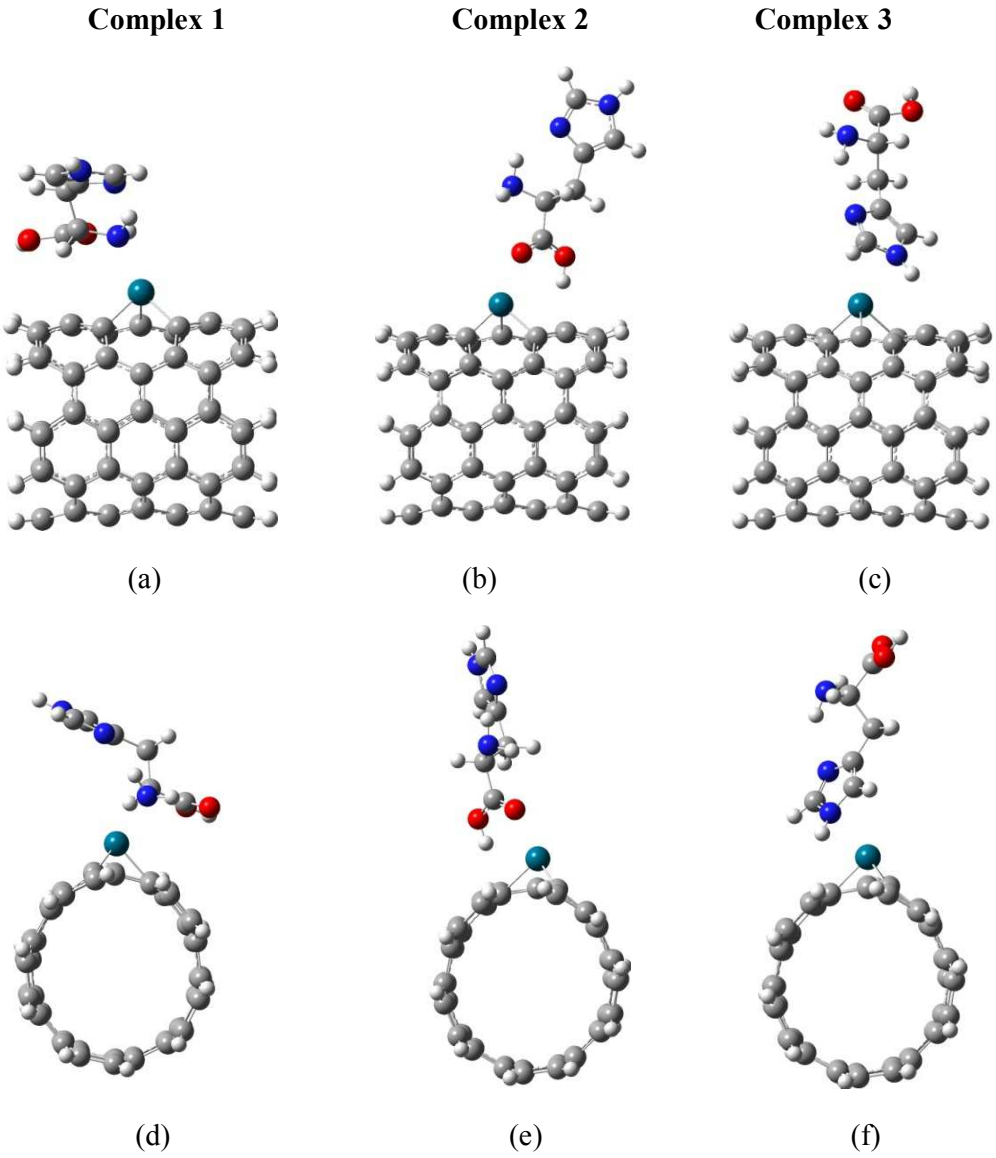

Fig. 3. His adsorbed Pd/SWCNT optimized complexes side view panels (a) from amine site, (b) from carbonyl site and (c) from ring site and panels (d), (e) and (f) corresponding sites from tope view

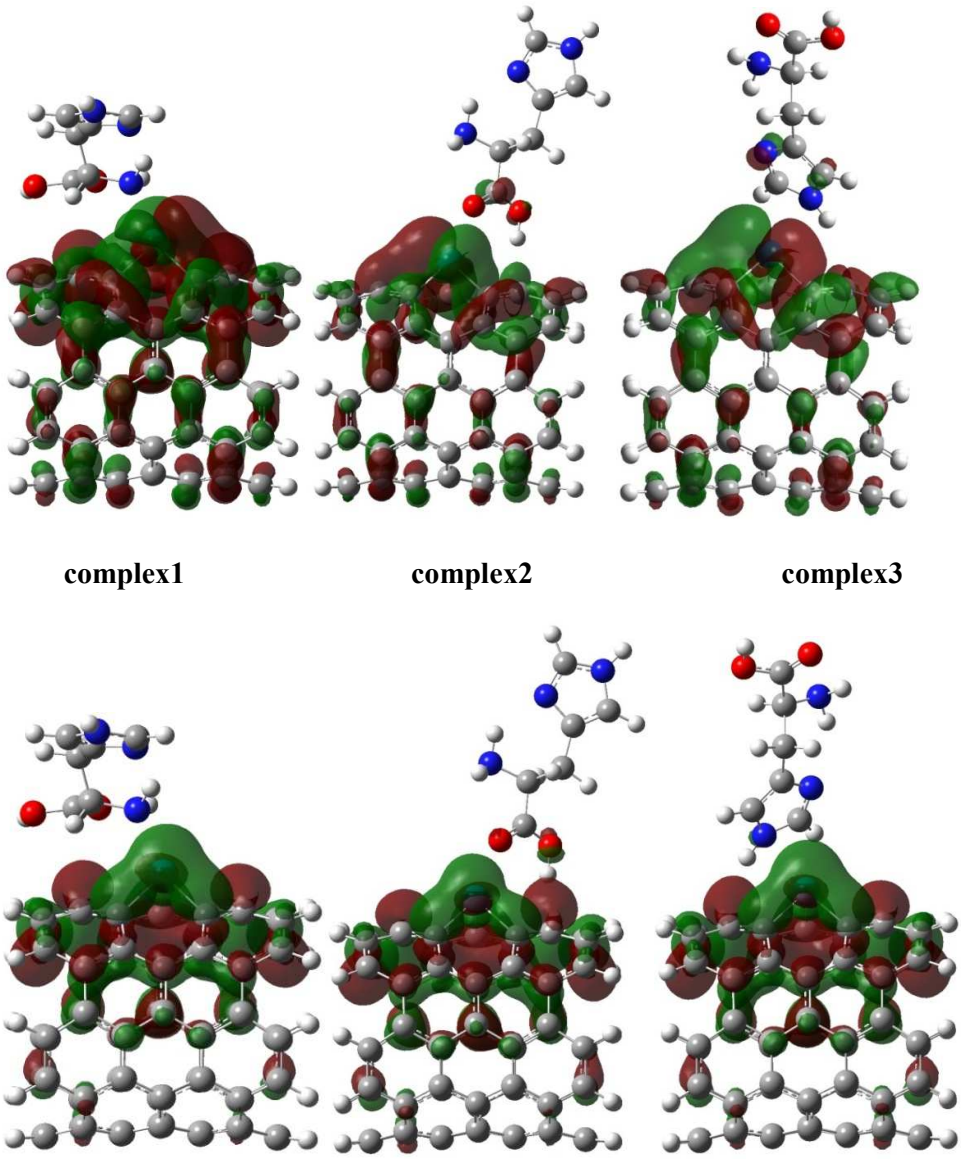

complex1 **complex2** **complex3**

Fig. 4. HOMO and LUMO plots of different comlpexes obtained with B3LYP/6-31g* level of theory

Table1. Adsorption energy (E_{ads},eV), interatomic distances, and topological parameters for studied His-Pd/SWCNT complexes

Complex 1

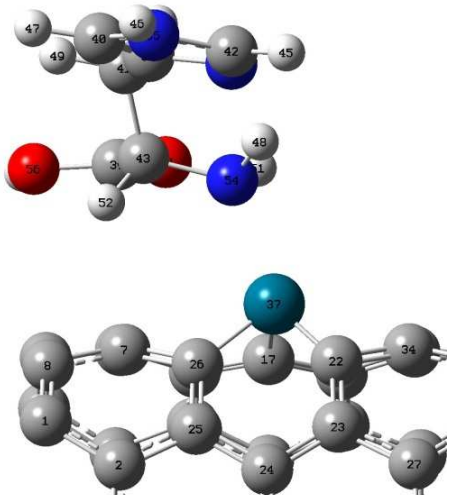

***E_{ads}*= -18.21**

Bond	Distance(Å)	ρ_{BCP}	$\nabla^2\rho_{BCP}$	ρ_{RCP}	$\nabla^2\rho_{RCP}$
Pd-C_{26}	2.004	0.1364	0.17	0.0170	0.10
Pd-C_{22}	1.980	0.1274	0.14	0.1428	0.08
pd-C_{17}	2.080	0.1099	0.12	0.0170	0.10
Pd-N_{54}	2.336	0.0571	0.22	-	-
N_{54}-C_{43}	1.480	0.2610	0.18	-	-
N_{54}-H_{48}	1.026	0.3240	-1.61	-	-
N_{54}-H_{51}	1.023	0.3220	-1.40	-	-

Table2. Adsorption energy (E_{ads},eV), interatomic distances, and topological parameters for studied His-Pd/SWCNT complexes

Complex 2

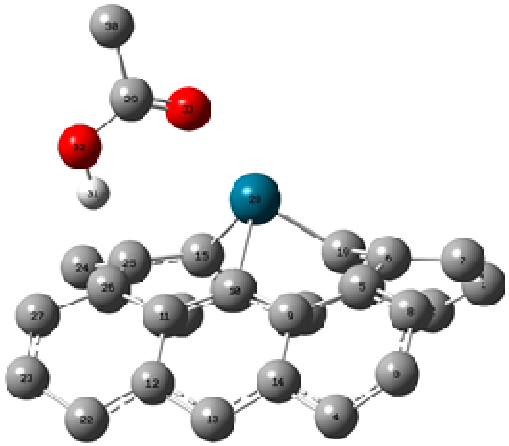

***E_{ads}*= -18.06**

Bond	Distance(Å)	ρ_{BCP}	$\nabla^2\rho_{BCP}$	ρ_{RCP}	$\nabla^2\rho_{RCP}$
Pd-C_{27}	1.979	0.1366	0.16	0.0171	0.01
Pd-C_{18}	2.068	0.1122	0.11	0. 1400	0.08
pd-C_{23}	2.002	0.1281	0.14	0.0180	0.01
Pd-O_{54}	2.287	0.0495	0.25	0.0059	0.01

Table3. Adsorption energy (E_{ads},eV), interatomic distances, and topological parameters for studied His-Pd/SWCNT complexes.

Complex 3

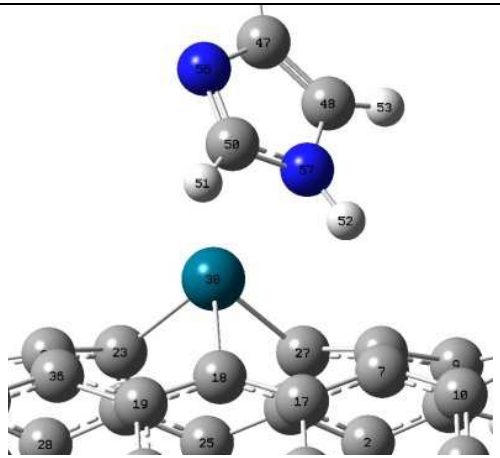

E_{ads}= **-17.57**

Bond	Distance(Å)	ρ_{BCP}	$\nabla^2\rho_{BCP}$	ρ_{RCP}	$\nabla^2\rho_{RCP}$
Pd-C_{23}	1.978	0.1299	0.1468	0.0177	0.10
Pd-C_{27}	1.994	0.1354	0.1576	0. 137	0.08
pd-C_{18}	2.068	0.1128	0.1202	0.0169	0.10
Pd-N_{57}	2.630	0.0284	0.0969	-	-
N_{57}-H_{52}	1.020	0.3196	-1.6120	0.0528	0.42

Table4. The highest occupied molecular orbital (HOMO) energy, ε_{HOMO}, the lowest unoccupied molecular orbitals (LUMO) energy, ε_{LUMO}, energy gap ε_{gap}, chemical potential, μ, chemical hardness, η and Fermi level energy, ε_F, (all values are in eV) for different investigated configurations.

Configuration	ε_{HOMO}	ε_{LUMO}	ε_{gap}	μ	η	ε_F
His	-5.904	-0.394	5.510	-3.149	2.755	-3.149
Pd/SWCNT	-4.155	-2.543	1.612	-3.349	0.806	-3.349
Complex1	-3.752	-2.104	1.648	-2.928	0.824	-2.928
Complex2	-4.000	-2.301	1.700	-3.150	0.850	-3.150
Complex3	-4.233	-2.547	1.687	-3.390	0.843	-3.390

Table5. NBO analysis of some important orbital interactions of studied complexes (intermolecular and intramolecular threshold energy for printing: 4 kcal/mol)

complex 1			**Complex2**			**Complex3**		
Donor	Acceptor	$E^{(2)}$	Donor	Acceptor	$E^{(2)}$	Donor	Acceptor	$E^{(2)}$
σH 22 - N 24	LP*(7)Pd	4.79	LP (1) C26	LP*(1) H31	51.89	LP (1) N36	LP*(5) Pd	6.23
LP (1) N 24	LP*(5)Pd	28.21	LP (1) O33	LP*(6)Pd	10.38	LP (1) N36	LP*(8) Pd	4.39
LP (1) N 24	LP*(7)Pd	18.91	LP (1) O33	LP*(7)Pd	9.77			
LP (1) N 24	σ*C6 -Pd	4.99	LP (2) O33	LP*(5)Pd	11.57			
			LP (2) O33	LP*(6)Pd	5.81			
			LP (2) O33	LP*(7)Pd	17.99			
			LP (2) O33	σ* C19 -Pd	6.13			
			σC 92 - O32	LP*(1) H31	12.77			
			LP (1) O32	LP*(1) H31	15.11			
			LP (3) O32	LP*(1) H31	429.57			
			LP*(1) H31	LP*(7)Pd	10.13